Evaluation of thermal insulation capacity and mechanical performance of a novel low-carbon thermal insulating foam concrete

Shi, Jinyan; Zhang, Minghu; Zhu, Xuezhen; Yalçınkaya, Çağlar; Çopuroğlu, Oğuzhan; Liu, Yuanchun

DOI
10.1016/j.enbuild.2024.114744

Publication date
2024

Document Version
Final published version

Published in
Energy and Buildings

Energy & Buildings 323 (2024) 114744

Contents lists available at ScienceDirect

Energy & Buildings

journal homepage: www.elsevier.com/locate/enb

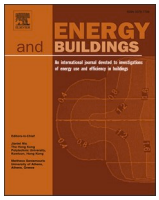

Evaluation of thermal insulation capacity and mechanical performance of a novel low-carbon thermal insulating foam concrete

Jinyan Shi [a], Minghu Zhang [a], Xuezhen Zhu [a,*], Çağlar Yalçınkaya [b], Oğuzhan Çopuroğlu [c], Yuanchun Liu [d]

[a] School of Civil Engineering, Central South University, Changsha 410075, China
[b] Department of Civil Engineering, Faculty of Engineering, Dokuz Eylül University, İzmir, Turkiye
[c] Faculty of Civil Engineering and Geosciences, Delft University of Technology, Delft, the Netherlands
[d] School of Water Conservancy and Civil Engineering, Northeast Agricultural University, Harbin 150030, China

ARTICLE INFO

Keywords:
Foamed concrete
Desert sand
Rice husk ash
Sustainability analysis
Insulation materials

ABSTRACT

The use of building insulation materials is an effective measure to reduce building energy consumption. To improve the sustainability of insulation materials, desert sand (DS) was used to replace part of the binder, and rice husk ash (RHA) was incorporated to further improve the performance of foamed concrete. The fresh properties, strengths, thermal properties and thermal insulation function of DS-based foamed concrete (DSFC) were systematically investigated. The use of DS and RHA to replace part of Portland cement (PC) and fly ash reduces the flowability of the mixture when the water/binder (PC, fly ash, DS and RHA) ratio is constant. Although the incorporation of DS into foamed concrete increases its density and thermal conductivity, it improves the volume stability of the sample. The strength of specimen with DS decreases due to the low reactivity of DS, which also reduces the content of hydration products. Further incorporation of RHA not only improves the matrix strength by increasing the C-S-H content but also improves the pore structure of the DSFC by increasing the yield stress of the paste. The joint application of DS and RHA effectively reduces the heat storage coefficient and thermal inertia index of DSFC, which is beneficial to improve the thermal insulation capacity of buildings and reduce energy consumption. Incorporating DS and RHA can effectively improve the environmental and economic benefits of the foamed mixture, and the unit strength cost and carbon emission per cubic meter of the 5%–10% RHA-modified samples are reduced by 20.3%–39.1% and 20.2%–38.9%, respectively, compared with the DS35. This research provides a new approach and theoretical basis for building energy saving and external wall insulation.

1. Introduction

Nowadays, concrete materials are still the most used building materials in the world, which are mainly composed of cement, aggregates, additives, and water. Ordinary Portland cement (OPC) is still the dominant binder in concrete products, but its annual production of CO_2 accounts for 7 %–8% of anthropogenic CO_2 emissions [1]. Every ton of OPC produced produces 0.98 tons of CO_2 [1]. As a result, OPC has become a major contributor to carbon emissions in the construction industry, which is not in line with a carbon–neutral strategy. Therefore, researchers have to develop multi-component binders to reduce the use of OPC [2,3]. In addition, concrete consumes a lot of natural resources such as river sand. Due to dwindling reserves of natural resources and the regulation of the Chinese government on river sand mining, researchers have had to find new alternative materials.

There are more than 6000000 km^2 of deserts in the world, of which China has 1533000 km^2, which contains rich desert sand (DS) resources [4]. Meanwhile, the desert area in China is still increasing at a rate of 560 km^2/year due to human activities [5]. Using DS to produce concrete materials is an acceptable strategy in some regions due to the scarcity of natural resources and the desertification in desert areas. For example, 61.3 % of the Rajasthan State in India is desert, and the cost of raw materials of concrete in desert areas is 1.1–1.5 times that of other areas [6,7]. In addition, like river sand, the main components of DS are Al_2O_3 and SiO_2, but its particle size is finer [5]. In general, DS is adopted as a partial replacement for river sand in concrete, which may improve the

* Corresponding author.
E-mail address: 18205162017@163.com (X. Zhu).

https://doi.org/10.1016/j.enbuild.2024.114744
Received 9 November 2023; Received in revised form 15 June 2024; Accepted 30 August 2024
Available online 1 September 2024

pore structure of the concrete due to the finer size [5]. However, high levels of DS affect the flowability of the mixture, which is often not recommended [5]. Therefore, some researchers use DS as a binder in concrete. Guettala et al. improved the strength of concrete using fine DS as a potential supplementary cementitious material (SCM, 5 %–15 %) [8]. Meanwhile, studies have also proved that under an alkaline environment, the dissolution of SiO_2 and CaO in fine DS participated in the hydration reaction [9]. Therefore, using fine DSs as a potential SCM is also a feasible solution [5]. Replacing some of the cement with SCM is one of the feasible strategies to reduce CO_2 emissions. Industrial by-products such as fly ash (FA) and slag are the most common SCMs and are widely used in concrete. However, due to the rising demand for SCM from concrete and the gradual closure of thermal power plants and steel mills due to high environmental pollution, there is a shortage of SCM prepared from industrial by-products in some countries [10]. On the other hand, in some underdeveloped areas, the reserves of industrial waste are very small. As a result, researchers have had to look for alternative SCMs. Agricultural products are more indispensable than industrial products, and their reserves increase with the increase in population. A large number of agricultural by-products are produced during the processing of crops, and researchers are trying to use them directly or after calcination in concrete [11]. Rice is an important crop, and the global annual output of rice is about 800 million tons, while China's annual output exceeds 200 million tons [12]. In the process of rice milling, a large amount of rice husks is produced, which has the potential for biomass power generation. In China, rice husks are used in biomass power plants, and 20 wt% of the rice husk ash (RHA) is retained [13,14]. The main component of RHA obtained at a specific temperature and environment is active silica, which is considered to be a silica fume-like SCM. Desina et al. reported that replacing cement with RHA could increase compressive strength by 45 % [15]. He et al. used RHA to replace 20 % of the cement and found that the strength of the specimen increased by about 10 %, which was attributed to the high pozzolanic reactivity and filling effect of RHA [16]. Meanwhile, the internal curing effect of RHA also improved the volume stability of concrete. In addition, the incorporation of RHA into the cement mixture can also improve its viscosity due to its high porosity and specific surface area [17]. Therefore, RHA is considered as a novel SCM with high reactivity and high reserves.

Building energy consumption is still the main part of energy consumption, which accounts for about 36 % of global energy consumption [18,19]. The application of building exterior wall thermal insulation materials is one of the main strategies to reduce building energy consumption. Lightweight foamed concrete has become a common external wall insulation material due to its excellent durability and low thermal conductivity [20,21]. In general, to reduce the density of foamed concrete and improve the stability of the fresh mixture, coarse aggregates are excluded, which means a higher binder content in the mixture [21]. In response to this phenomenon, this study considers using DS to replace binders to relieve the high carbon emission and insufficient reserves of binder in foamed concrete. However, there are no relevant reports on DS-based foamed concrete (DSFC). This is because that the incorporation of DS into foamed concrete leads to the increase of apparent density, which is not conducive to the heat storage capacity of foamed concrete. In order to solve this problem, this study uses the combination of RHA and DS to prepare a novel foamed concrete, which not only reduces the density of foamed concrete, but also improves its mechanical properties. Finally, this study conducts a comprehensive evaluation of RHA-modified DSFC in terms of technical indicators, economic and environmental impact, and compares it with traditional OPC-based foamed concrete.

2. Materials and experiments

2.1. Materials

OPC, FA, and RHA are adopted as the main binder, and DS is used to replace part of the binder due to its finer particles. Grade 42.5 OPC is provided by Pingtang Cement Plant, and its main chemical composition is presented in Table 1. To increase the fluidity of the mixture, class I FA is used, which is supplied by Rongchangsheng Materials Co., Ltd. RHA is obtained by burning rice husks in a high-temperature furnace (1 h, 600 ℃). The DS comes from the Mu Us Desert land in Yanchi County, Ningxia, and its fineness modulus is 0.292 (See Fig. 1). The polycarboxylate superplasticizer (SP) is provided by Qinfen Building Materials, and its water-reducing ratio is about 25 %. In addition, manganese dioxide, sodium nitrite, sodium pyrophosphate, and calcium stearate (CS) are all chemical analytical grades provided by Hunan Huihong Co., Ltd. The particle size distribution of the material is presented in Fig. 2, and RHA is significantly finer than OPC.

2.2. Mix proportions and specimens preparation

A typical mix proportion of OPC-based foam concrete was adopted, as presented in Table 2 [22]. To control the hydration exotherm of the mixture and prevent it from collapsing and cracking, the weight ratio of OPC and FA was set at 1.23:1. Hydrogen peroxide and manganese dioxide were adopted as chemical foaming agent and catalyst, respectively, and the weight ratio of the two was set to 10:1 and remained unchanged in all mixtures. SP was used to improve the fluidity of the mixture, which makes it easier for air bubbles to be generated and can be distributed evenly. Meanwhile, CS was used as a foam stabilizer, and sodium nitrite was used as a coagulant to prevent the DSFC from collapsing, and their dosage was 0.28% and 4.29% of binders, respectively. Sodium pyrophosphate can improve the stability of hydrogen peroxide and slow down its decomposition rate, and its weight ratio to CS was set to 1:1. Moreover, due to the shortage of water resources in desert areas, cement plants and power plants are located far away, resulting in a high transportation cost of binders. Meanwhile, the insufficient reserves of FA caused by low-carbon policies results in the requirement to find an alternative material. As a nature source, DS is abundant in desert areas, and has low cost and low carbon emissions. Therefore, DS was used to replace the binder (OPC and FA), and the substitution levels were 20 %, 35 %, and 50 %, respectively. To further improve the performance of DSFC, RHA was used to replace part of OPC and FA, and the substitution ratio was 5 %–15 %. In addition, the water/binder (OPC+FA+DS+RHA) ratio was set to 0.41.

First, the solid material (OPC, FA, DS, RHA, $NaNO_2$, CS, $Na_4P_2O_7{\cdot}10H_2O$, and MnO_2) were stirred well, and then half of the aqueous solution (water and SP) was poured into the mixture until well stirred (See Fig. 3). The residual aqueous solution was then incorporated to the mixture and stirred at low speed for 30 s, then high speed for 10 s. To prevent bubbles from overflowing, H_2O_2 was added to the mixture last, and the stirring time was 10 s. The mixture was quickly poured into moulds and demolded after air curing for 24 h, and then further cured under standard curing conditions.

3. Test methods

3.1. Fresh properties

A fluidity cone with an upper diameter of 36 mm and a lower diameter of 60 mm was used to test the fluidity of the paste without foam according to previous studies [23]. The fresh paste was injected into the fluidity cone, and the fluidity cone was raised to allow the paste to flow freely, and the fluidity was tested after 60 s, as shown in Fig. 4(a). To accurately test the hindering effect of the paste on air bubbles, the rheological parameters of the paste were tested using the Anton Paar

Table 1
The chemical composition of binder (wt. %).

Type	CaO	SiO_2	Al_2O_3	Fe_2O_3	MgO	SO_3	K_2O	TiO_2	P_2O_5	Na_2O	LOI
OPC	62.1	21.18	7.16	3.50	2.01	2.56	–	–	–	–	2.40
FA	2.61	52.4	35.3	2.81	0.73	0.47	1.42	1.61	–	0.67	2.86
RHA	1.10	91.25	0.37	0.22	0.64	0.49	3.56	0.02	1.36	0.06	5.10

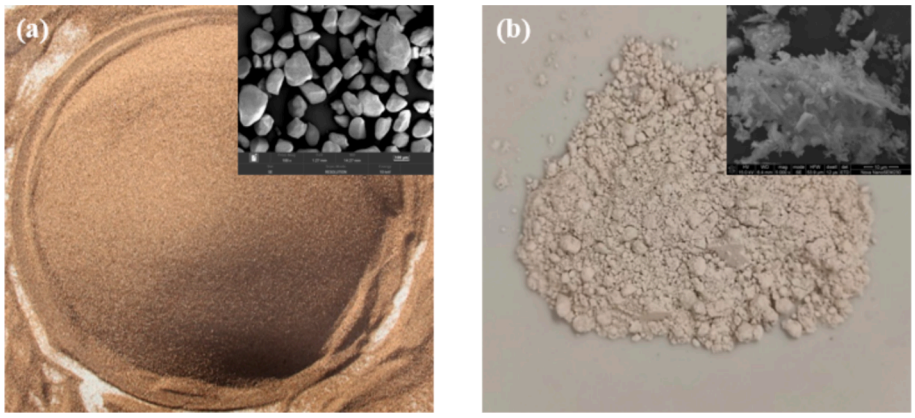

Fig. 1. The images of DS (a) and RHA (b).

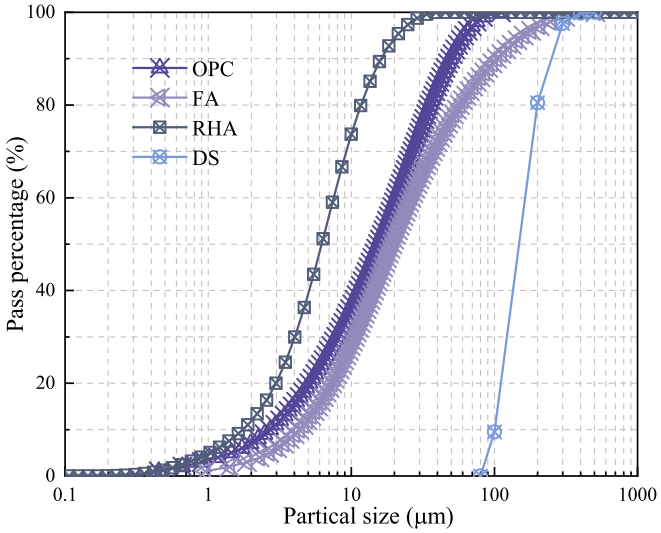

Fig. 2. Particle size distribution of DS and binder.

Table 2
The mix proportions for DSFCs .

Mix.	OPC+FA	DS	RHA
DS0	1	0	–
DS20	0.8	0.2	–
DS35	0.65	0.35	–
DS50	0.5	0.5	–
MR5	0.617	0.35	0.033
MR10	0.585	0.35	0.065
MR15	0.552	0.35	0.098

Rheolab QC rheometer (ST22-4 V-40). A common testing regime was adopted (See Fig. 4(b)), and the test results were fitted by a Bingham model [21].

3.2. Hardened performance

The compressive strength of the foamed concrete (100 × 100 × 100 mm) was tested and the loading rate was 0.6 kN/s. After the foamed concrete was dried in oven at 110°C to constant weight, its dry weight was measured to evaluate the dry density. The dry density of the specimens was the ratio of the mass and volume of the three dry specimens. The thermal conductivity of the foamed board was measured by the steady-state method, and the detailed procedure can be found in a previous study [18]. The thermal conductivity of the DSFC with a size of 200 × 200 × 20 mm was tested by the DRH-III device with the temperature of 15 and 35 ℃ on both sides. According to ASTM C596, the drying shrinkage of foamed concrete was tested up to 90 d at a test humidity and temperature of 60 ± 5 % and 20 ± 2 ℃, respectively. The length change of the sample was monitored by a dial gauge to assess its risk of shrinkage cracking.

3.3. Pore structure and microstructure

The pore structure of DSFC samples was tested by image processing, and the detailed experimental procedure can be found in a previous study [23]. The DSFC sample (40 × 40 × 40 mm) was cut from the middle, and the cross-sectional images were collected by a camera, then the pore structure parameters were acquired by the image-pro plus software. During image processing, the acquired images were binarized, and parameters such as pore diameter and area were counted, as shown in Fig. 5. In order to improve the accuracy of test results, three samples were applied.

Samples were cut from the DSFC and soaked in isopropanol, and then vacuum dried over 7 d. The dried specimen surface was sprayed with gold and used for the scanning electron microscope (SEM) test (TESCAN MIRA 4). Meanwhile, the dried specimens were ground into powder for Thermogravimetry (TG) testing, and the specimens were heated from 30 to 1000 ℃ under a N_2 atmosphere. For quantitative analysis of hydration product content, non-evaporative water content (NEW, W_{NEW}) and calcium hydroxide (W_{CH}) content were calculated through Eqs. (1) and (2). Further, X-ray diffraction (XRD) was adopted to identify the phase composition in DSFC, and the determination angle (2θ) range is 5°–60° with a speed of 10°/min. In addition, FTIR was also adopted to characterize functional groups in the DSFC sample, and the wave test range

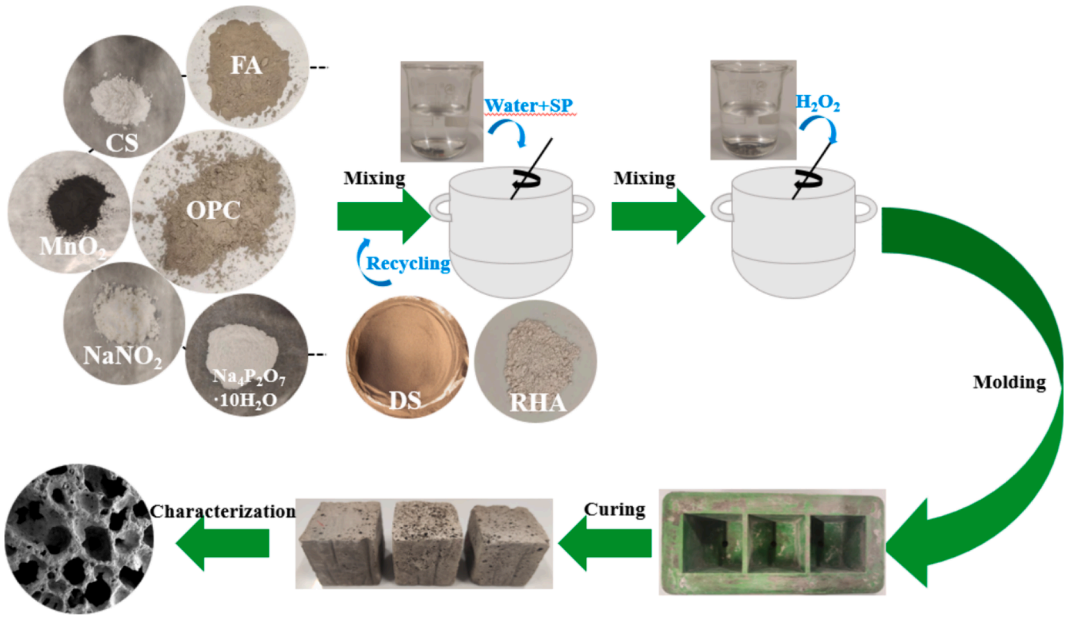

Fig. 3. The preparation process of DSFC.

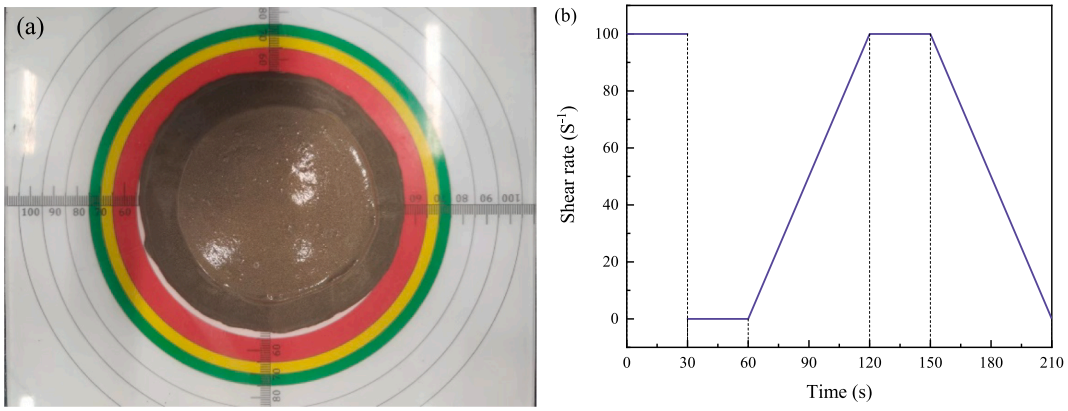

Fig. 4. Fluidity test of DSFC paste.

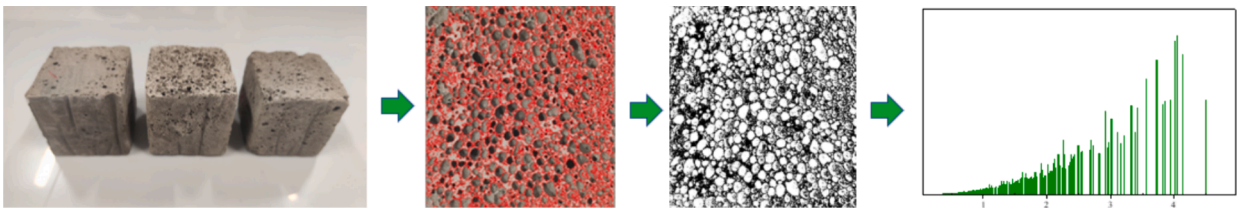

Fig. 5. Image processing process.

was between 500 and 4000 cm^{-1}.

$$W_{NEW} = \left(\frac{m_{50} - m_{1000}}{m_{50}} - (f_C \times LOI_C + f_{DS} \times LOI_{DS} + f_{FA} \times LOI_{FA} + f_{RHA} \times LOI_{RHA})\right) \times 100\% \quad (1)$$

$$W_{CH} = \left(\frac{m_{380} - m_{460}}{m_{Total}} \times \frac{74}{18} + \frac{m_{460} - m_{760}}{m_{Total}} \times \frac{74}{44}\right) \times 100\% \quad (2)$$

Where, m_{50}, m_{380}, m_{460}, m_{760}, and m_{1000} represent the mass of DSFC at 50, 380, 460, 760, and 1000 ℃, respectively, μg. m_{Total} represents the unheated mass of the sample, μg. LOI_C, LOI_{FA}, LOI_{DS}, and LOI_{RHA} represent the LOI of OPC, FA, DS, and RHA, respectively. f_C, f_{FA}, f_{DS}, and f_{RHA} represent the weight fraction of OPC, FA, DS, and RHA in the cementitious material, respectively.

4. Results

4.1. Fluidity

The fluidity of the paste is a key factor controlling the stability of DSFC. Excessive fluidity of paste will accelerate the rise, aggregation, and overflow of bubbles [21]. However, pastes with too low fluidity do

not fully encapsulate the air bubbles, causing them to overflow. Under the condition that the water/binder (OPC+FA+DS+RHA) ratio remained unchanged, with the increase of DS content, the fluidity of the paste decreased obviously, as shown in Fig. 6. When the DS substitution level was 50 %, its fluidity was reduced by 15.36 % relative to the plain paste. Although DS is used as an inert filler, its particle size is fine and its high specific surface area consumes some free water. In order for the mixture to flow, the paste wraps around the DS surface, which also reduces the fluidity of the mixture. Meanwhile, the incorporation of RHA (from 0 % to 15 %) also reduced the fluidity of the mixture from 102 to 82 mm. Compared to OPC and FA, the particle size of RHA is finer and its porous structure increases its water demand. Therefore, the incorporation of RHA decreased the flowability of the mixture, but the reduction value was not significant.

4.2. Rheological parameters

The dynamic yield stress and plastic viscosity (Y&P) were obtained by fitting Bingham model as presented in Fig. 7. The Y&P of the paste are the main indicators for controlling the generation, movement, and collapse of bubbles in the mixture. The higher Y&P can prevent the overflow and movement of air bubbles when the fluidity of the mixture is satisfactory. However, excessively high Y&P also affect the fluidity of the mixture, which in turn affects the formation of new bubbles. When a small amount of DS was incorporated into the paste, Y&P of the mixture decreased slightly, which is a shear-thinning phenomenon [24,25]. Under shear action and self-weight, DS causes the flocculation structure of the cement paste to be destroyed, thereby increasing the free water content and increasing Y&P. With the further increase of DS content, the paste content required to encapsulate DS increases significantly, which leads to a significant increase in Y&P of the mixture. The incorporation of 50 % DS resulted in an excessively high Y&P of the mixture, which is detrimental to the formation of initial stable bubbles. Further, increasing the RHA content increased the Y&P of the mixture. Properly increasing the Y&P of the paste can effectively prevent the bubbles from moving, converging, and breaking in the system, thereby preparing foamed concrete with an excellent pore structure [21].

4.3. Dry density

The 28-d dry density of DSFC was between 499.80 and 579.70 kg/m^3, which clearly falls into the category of lightweight foamed concrete, as presented in Fig. 8. The 28-d dry density of plain foamed concrete (DS0) was 524.73 kg/m^3, while those of the DSFC with 20 %, 35 %, and

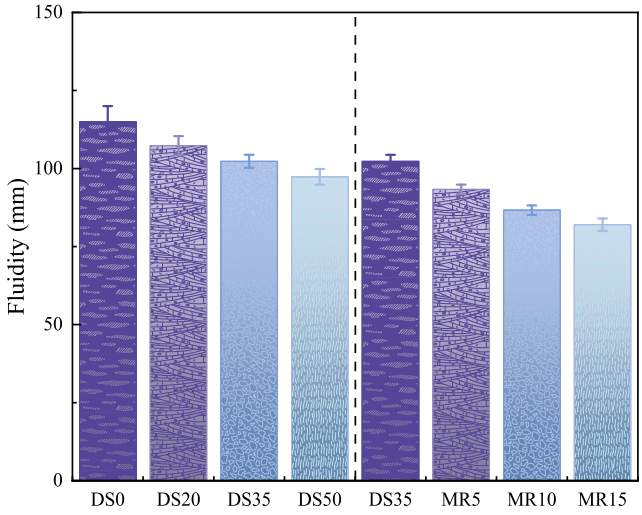

Fig. 6. The fluidity of DSFC paste.

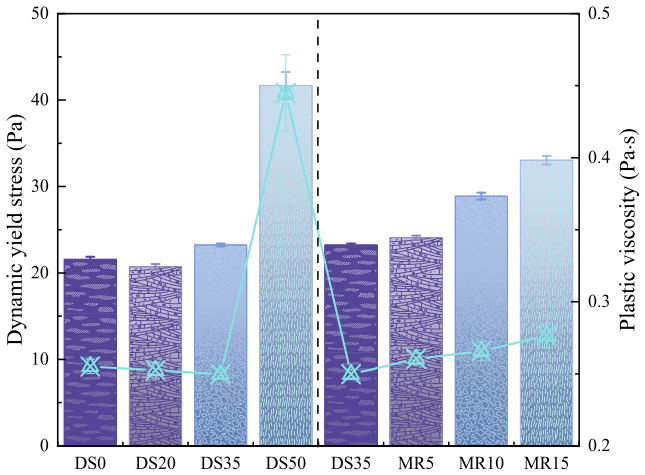

Fig. 7. The rheological parameters of the DSFC paste.

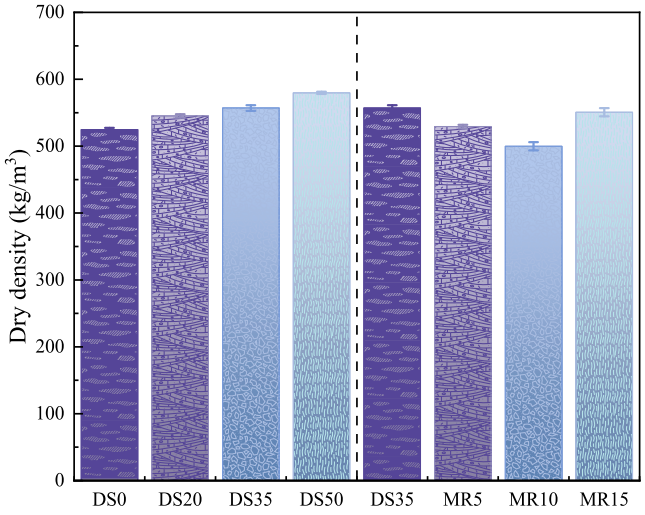

Fig. 8. Dry density of DSFC specimen at 28 d.

50 % DS were 545.13, 557.03, and 579.70 kg/m^3, respectively corresponding to approximately 3.89 %, 6.16 %, and 10.48 % increase compared to that of the DS0. When OPC and FA were replaced by DS with higher density, the dry density of DSFC increased significantly. Meanwhile, the air content is closely related to the density of hardened DSFC. In DSFC, the fresh paste was encapsulated on the DS surface. Therefore, as the DS substitution level increased, the flowable paste content decreased relatively. On the other hand, the Y&P of the mixture increased substantially. This all resulted in a reduction in air bubble content due to less paste volume. Thus, it was difficult to encapsulate the air bubbles and prevent them from overflowing. For RHA-modified DSFCs, the dry density first decreased and then increased, and reached a minimum value when the RHA content was 10 %. When 10 % of OPC and FA were replaced by RHA, the dry density of DSFC was only 499.8 kg/m^3, which was 10.27 % lower than that of the DS35 sample. RHA is a porous material with a significantly lighter density than OPC and FA. As shown in Fig. 8, the incorporation of RHA increased the Y&P of the paste. Properly increasing the Y&P of the paste can effectively prevent the bubbles from overflowing and improve the pore structure of the specimen [21].

4.4. Compressive strength

The effects of DS and RHA content on the strength of DSFC specimens

are shown in Fig. 9. For the DS0, its 7-d and 28-d strengths were 3.20 and 3.63 MPa, respectively, which meet the requirements of external wall insulation materials. Replacing OPC and FA with DS reduced the matrix strength of DSFC due to its lower reactivity. Meanwhile, the content of DS also has a significant effect on the pore structure of DSFC, which is another important factor controlling the strength of DSFC. Too high DS content reduced the fluidity of the mixture and significantly increased its Y&P, which made it difficult for the newly generated initial bubbles to be completely encapsulated. This may exacerbate the overflow and coalescence of bubbles, resulting in a decrease in sample strength. Therefore, the 7-d and 28-d compressive strengths of DSFC mixed with 50 % DS were only 34.38 % and 36.70 % of the control group, respectively. This reduction of compressive strength caused by incorporating DS is similar with the previous findings in literature [4]. However, unlike this research, incorporating 20 % DS as binder resulted in only reducing by 5 % of 28-d compressive strength of cement paste in literature [4], which is much lower than the loss ratio of compressive strength in this study. This phenomenon may be mainly due to the difference in particle size and chemical composition of DS. Kai et al. performed the screen work of DS and then used the fine particle (<75 μm) of DS as the SCM in cement paste [4]. In general, the fine DS has a greater filling effect and pozzolanic effect in cement-based material, which is beneficial to the strength development of cement paste. On the other hand, after screening, the SiO_2 content of fine DS (<75 μm) is only 50 % of that of original DS without screening [4]. The alumina, calcium oxide, magnesium oxide, and sulfur trioxide have a high proportion in DS, which also is beneficial to increase the hydration degree of cement paste.

As a highly reactive SCM, RHA is adopted to the DSFC system to compensate for the compressive strength reduction caused by the incorporation of DS. In the DSFC system, RHA reacts with CH to form C-S-H gel, which increases the mechanical properties of the specimens. Compared with DS35, the 7-d and 28-d compressive strength of MR15 increase by 15.6 % and 63.3 %, respectively. Meanwhile, RHA is a porous structure, which has an internal curing function in the DSFC system. In the DSFC system with a high water/binder ratio, RHA adsorbs the excess free water and releases them after the sample hardens, which effectively promotes the long-term hydration reaction of the sample. In addition, the incorporation of RHA increases the Y&P of the mixture, which also effectively prevents the generation of large-sized bubbles.

4.5. Drying shrinkage

Fig. 10 presents the drying shrinkage deformation of DSFC samples. Due to the higher porosity and larger pore size of foamed concrete, its drying shrinkage was more serious than that of ordinary concrete. Incorporating DS was an effective means to reduce the shrinkage deformation of DSFC. When the DS content was 50 %, the 90-d drying shrinkage value of the DSFC was only 62.96 % of that of the plain foamed concrete. This was mainly because, with the increase of the DS substitution ratio, the relative content of the binder decreased, thereby reducing the content of shrinkage components. The further incorporation of RHA reduced the drying shrinkage of DSFC samples. The 90-d shrinkage deformation of DSFC mixed with 35 % DS (DS35) was 2.75 mm/m, while those of the DSFC with 5 %, 10 %, and 15 % RHA were 2.45, 2.40, and 2.1 mm/m, respectively corresponding to approximately 10.91 %, 12.73 %, and 23.64 % decrease compared to that of the DS35. The internal curing effect of RHA can alleviate the water loss inside the sample, and it can improve the stiffness of DSFC, thereby effectively resisting shrinkage deformation.

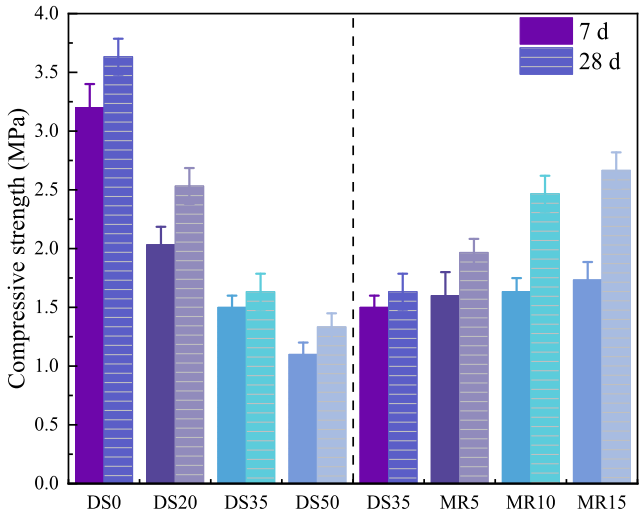

Fig. 9. The compressive strength of DSFC specimens.

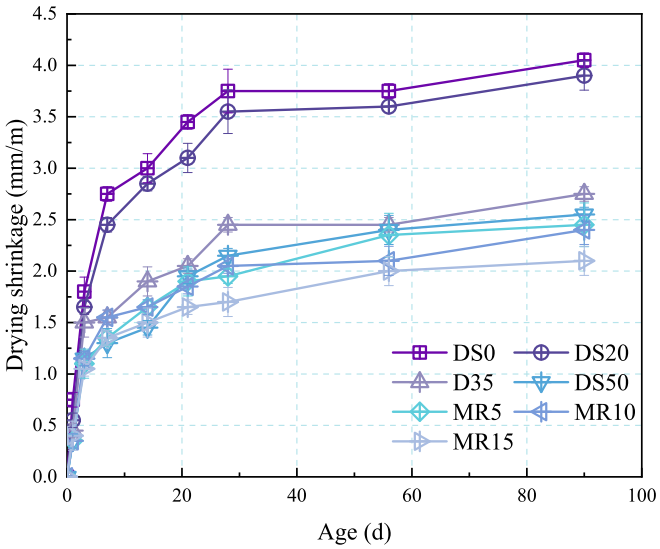

Fig. 10. Drying shrinkage of DSFC specimens.

4.6. Thermal conductivity

Fig. 11 presents the 28-d thermal conductivity of DSFC, which is one of the most important indicators for foamed concrete. The 28-d thermal conductivity of DSFC was between 0.095 and 0.160 W/m·k, which meets the performance requirements of external wall insulation materials, as presented in Fig. 11(a). With the increase of DS content, the thermal conductivity of DSFC increased significantly. This is closely related to the density of DSFC, as presented in Fig. 11(b). Generally speaking, the thermal conductivity of foamed concrete is positively correlated with its density. Incorporating DS increased the density of foamed concrete, and incorporating too much DS was not beneficial to the development of the sample's pore structure. Meanwhile, increasing RHA content, the thermal conductivity of DSFC first decreased and then increased. As a porous material, RHA can effectively reduce the density of DSFC and improve the heat transfer path inside the specimen. The thermal conductivity of DSFC reached the lowest value when the RHA content was 10 %, which was reduced by 20.86 % compared to the DS35 sample. Incorporating an appropriate amount of RHA into the DSFC system could increase the Y&P of the paste, which effectively prevented the coalescence of air bubbles and prepares fine pores. The fine pores increase the path for heat conduction, which reduces the thermal conductivity of the DSFC. However, the excessively high RHA content greatly reduced the fluidity of the mixture, which reduced the porosity of DSFC, increasing the thermal conductivity of the samples.

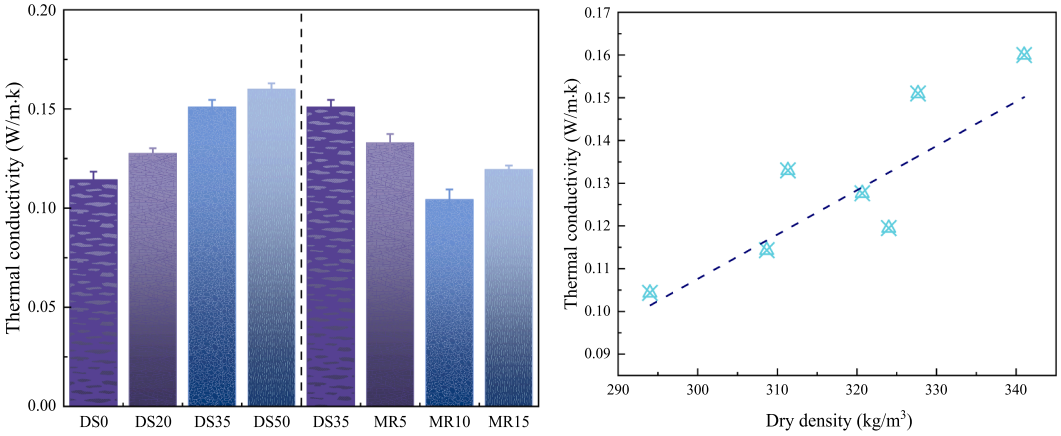

Fig. 11. The 28-d thermal conductivity of DSFC specimens.

4.7. Pore structure

The pore structure of foamed concrete is the main factor that determines its strength and thermal insulation performance. Fig. 12 presents the cross-sectional images of the DSFC samples and the pore structure obtained by image processing techniques is given in Fig. 13. Due to the higher fluidity of the plain pastes, this makes it easier for air bubbles to aggregate and form large-sized pores in the hardened samples (DS0 in Fig. 12). The incorporation of DS to foamed concrete reduced the fluidity of the mixture, which inhibited the movement of air bubbles. However, the density difference between the DS and the paste caused the DS to subsidence, which disturbs the stability of the bubbles. Therefore, the pore homogeneity in the images of the DS35 sample was significantly increased. Further incorporation of RHA increased the plastic viscosity of the foamed mixture, thereby improving the pore structure of the hardened samples. Some small and uniform pores can be found in the RH10 sample, which is also the key to its excellent performance.

The content of DS had a significant effect on the pore size distribution of foamed concrete, as shown in Fig. 13. Due to the lower Y&P of the DS0 pastes, this led to an increase in the number of large-sized bubbles. In low-viscosity fluids, chemical foaming is more likely to generate small-sized initial bubbles, but it is difficult to maintain the bubbles from moving, fusing, and collapsing. Under the combined action of the drainage force, buoyancy force, and confinement force of the bubble, the low yield stress is difficult to provide sufficient resistance, which makes the bubbles gradually merge and float up. Therefore, the pores of the DS0 sample were mainly distributed in the interval with a size higher than 1.8 mm. After the incorporation of 35 % DS, the Y&P of the mixture increased, which shifted the pores to smaller sizes. Of course, the reduction in pore size and porosity is also related to the shearing effect of DS in the foamed mixture. The DS moving downwards has a higher probability of encountering large-sized bubbles, which may have a cutting effect on them. On the other hand, the sedimentation of DS also exacerbates the floating of large-sized bubbles. When the content of DS was 50 %, its porosity was reduced by 14.95 % compared to the plain sample. This is mainly because the excessive yield stress limits the generation of new bubbles, and the weak encapsulation ability reduces the gas retention ratio [21].

Fig. 14 shows the effect of RHA content on the 28-d pore size distribution of DSFC samples. Appropriate incorporation of RHA not only improved the matrix strength but also improved the pore structure of DSFC, which was related to the reactivity of RHA and its effect on the improvement of rheological parameters of OPC-based paste. Properly increasing the Y&P of the mixture can prevent the transformation of small-sized bubbles to large-sized bubbles, and the floating and overflowing of bubbles. Therefore, the porosity of large-sized pore was significantly reduced in the DSFC sample mixed with 10 % RHA, and it shifted to small-sized pores. For the MR10 sample, the porosity of pores larger than 4 mm was significantly lower than in the DS35 sample. Meanwhile, MR10 had no pores larger than 5 mm, which had a significant effect on its performance improvement. In addition, the high RHA content caused an increase in the Y&P of the DSFC mixture, which means that the paste does not have enough free water to encapsulate the bubbles when they are first formed. Therefore, excess RHA decreased the porosity of DSFC samples and coarsened the pore structure.

4.8. Microstructure

To further observe the pore structure and matrix compactness of

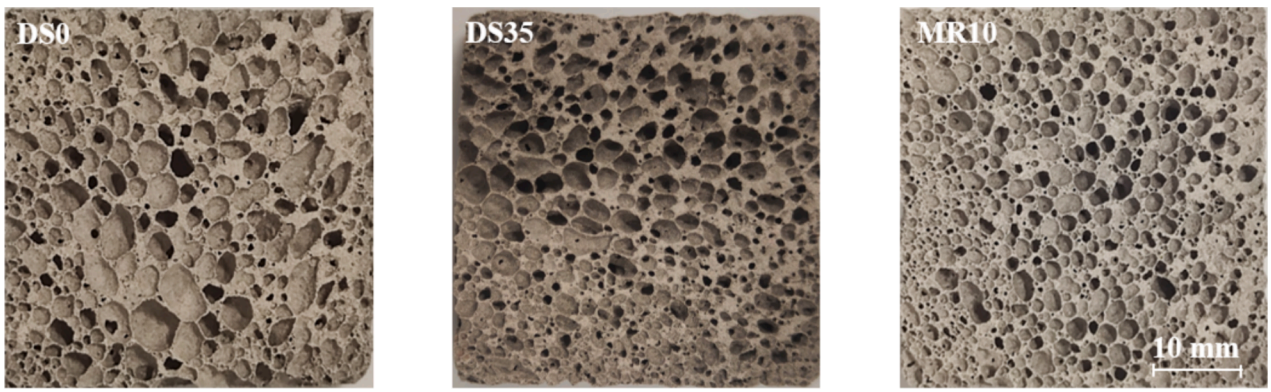

Fig. 12. The 28-d pore images of DSFC.

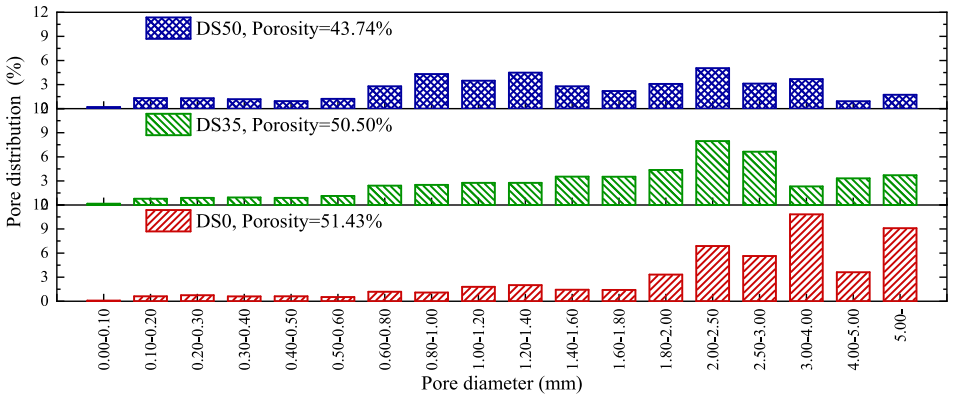

Fig. 13. The pore size distribution of DSFC at 28 d.

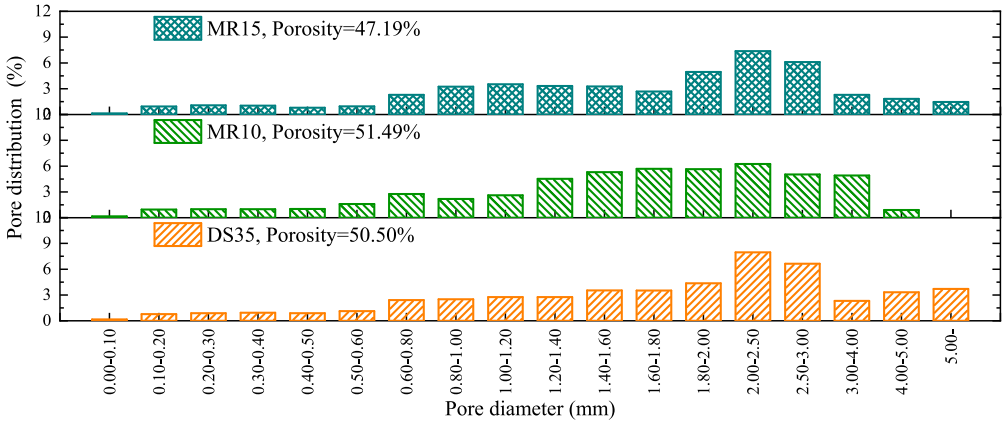

Fig. 14. The pore size distribution of DSFC at 28 d.

DSFC, SEM was used to observe the microstructure of the specimens, as shown in Fig. 15. Due to the higher fluidity of the DS0 mixture, its pore size was larger and its pore interconnectivity was higher, as shown in Fig. 15(a). High pore interconnectivity is detrimental to the strength development of foamed concrete and simplifies its heat transfer path. After further incorporating DS, the pore interconnectivity of DSFC was significantly reduced. The stability of the fresh foamed mixture was improved with increasing Y&P, thereby improving the pore structure of the hardened samples. When the content of RHA was 10 %, the pore size of DSFC was significantly reduced, and the pore interconnectivity was improved.

Besides pore structure, matrix compactness is another important indicator that affects sample performance. In DSFC, the paste layer was formed among the foams, which hindered the fusion of bubbles and acts as a skeleton, as presented in Fig. 16. The main hydration products (AFt, CH, and C-S-H gel) and reacted FA particles can be found on the matrix (Fig. 16(a)). The compactness of the matrix of DS-modified foamed concrete was obviously reduced due to the decrease in cement content. In addition, irregular DS particles (100–200 μm) can be found in DS35 samples, which have better compatibility with the cement matrix. This is mainly due to the potential pozzolanic reactivity of DS [5,8,26], which makes the interfacial transition zone between the DS and the cement matrix smaller. RHA is rich in active SiO_2, which can participate in the reaction to generate C-S-H gel, thereby increasing the compactness of the matrix (see Fig. 16(c)).

Fig. 17 presents the content of non-evaporable water (W_{NEW}) and calcium hydroxide (W_{CH}) of DSFC samples at 28 d. As presented in Fig. 17, the weight loss of 30–400 ℃ is related to the decomposition of C-S-H gel, AFt, and AFm. The mass loss of 380–460 ℃ is attributed to the decomposition of CH. Due to the high porosity and interconnectivity of foamed concrete, the $CaCO_3$ content in the samples was high (460–760 ℃). When DS was used to replace OPC and FA, both the hydration degree and $Ca(OH)_2$ content of the samples were significantly reduced, mainly because DS had little reactivity in this system. When the substitution ratio of DS reached 35 %, the W_{NEW} and W_{CH} of the sample were only 55.89 % and 61.01 % of those of the plain paste. RHA contains high content of amorphous SiO_2, which can react with CH to form C-S-H gel. Meanwhile, the internal curing effect of RHA also promotes the hydration of residual cement clinker and FA, thereby increasing the long-term hydration degree of the samples. Therefore, further incorporation of 15 % RHA into the DS35 mixture resulted in an increase in the W_{NEW} and a decrease in the $Ca(OH)_2$ content.

Fig. 18 shows the 28-d phase results for the DSFC sample. The plain paste mainly includes $CaCO_3$, $Ca(OH)_2$, AFt, and mullite from FA. When DS was incorporated into foamed concrete, the peak of the SiO_2 phase was significantly increased. This is mainly because the main component of DS is SiO_2, and its reactivity is very low. Due to the porous structure of DSFC, the carbonation is more serious, so it is difficult to judge the content of hydration products by the peak intensities of CH and $CaCO_3$. In addition, due to the incorporation of additives such as $NaNO_2$ and $Na_4P_2O_7{\cdot}10H_2O$ in the mixture, sodium calcium aluminum sulfate hydrate and calcium phosphate hydrate phases exist in the foamed concrete.

The vibrational bands of 794, 522, and 452 cm^{-1} are Si-O symmetric stretching, Si-O in-plane bending vibration (ν2) of silicate centered, and Si-O out-of-plane bending vibration (ν4) of silicate, respectively (See Fig. 19) [27]. Meanwhile, the vibrations occurring near 646 cm^{-1} are also related to Si–O–Si bond in C-S-H [28]. The 1797 and 2514 cm^{-1} are the vibration peaks of $CaCO_3$, and 873 and 1415 cm^{-1} are caused by the vibration of υ2 of CO_3 and CO_3, respectively [29]. Meanwhile, the

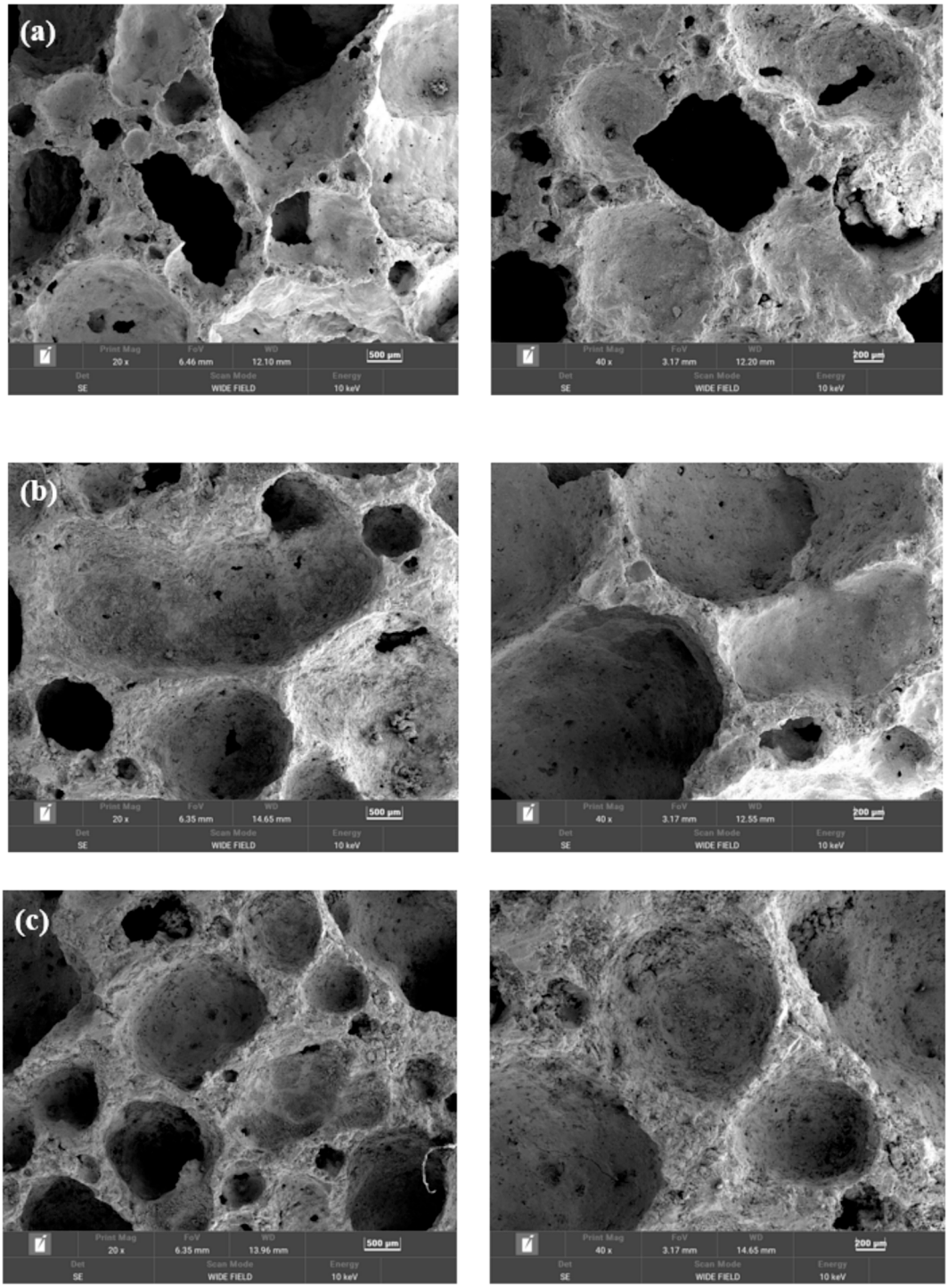

Fig. 15. The 28-d SEM images of DSFC samples. (a) DS0, (b) DS35, and (c) MR10.

vibration of the samples around 1649 and 3415 cm^{-1} is considered to be generated by υ2 and υ3 in the H_2O [29]. The vibrational peak of 3644 cm^{-1} is caused by CH, but its content is significantly lower due to the higher degree of carbonation of the specimen. There is a broad peak between 900 and 1115 cm^{-1} in the spectrum, which may be related to polymerized silica. Also, there are some small peaks below 800 cm^{-1}, which may be related to chemical additives. When DS was mixed into the mixture, the hydration product content of the specimens was significantly reduced. Relative to the DS35 sample, further incorporating RHA increased the C-S-H content, which is also similar to the TGA results.

5. Discussion

5.1. Thermal insulation function

The heat storage coefficient (S, $W/m^2 \cdot K$) and thermal inertia index (D) are used to evaluate the thermal insulation function of the DSFC board. The heat storage coefficient is generally used to characterize the heat storage capacity of the envelope structure material [30]. The thermal inertia index refers to the temperature fluctuation degree on the other side when one side of the material board is subjected to periodic harmonic heating effects, which are calculated by Eqs. (3) and (4).

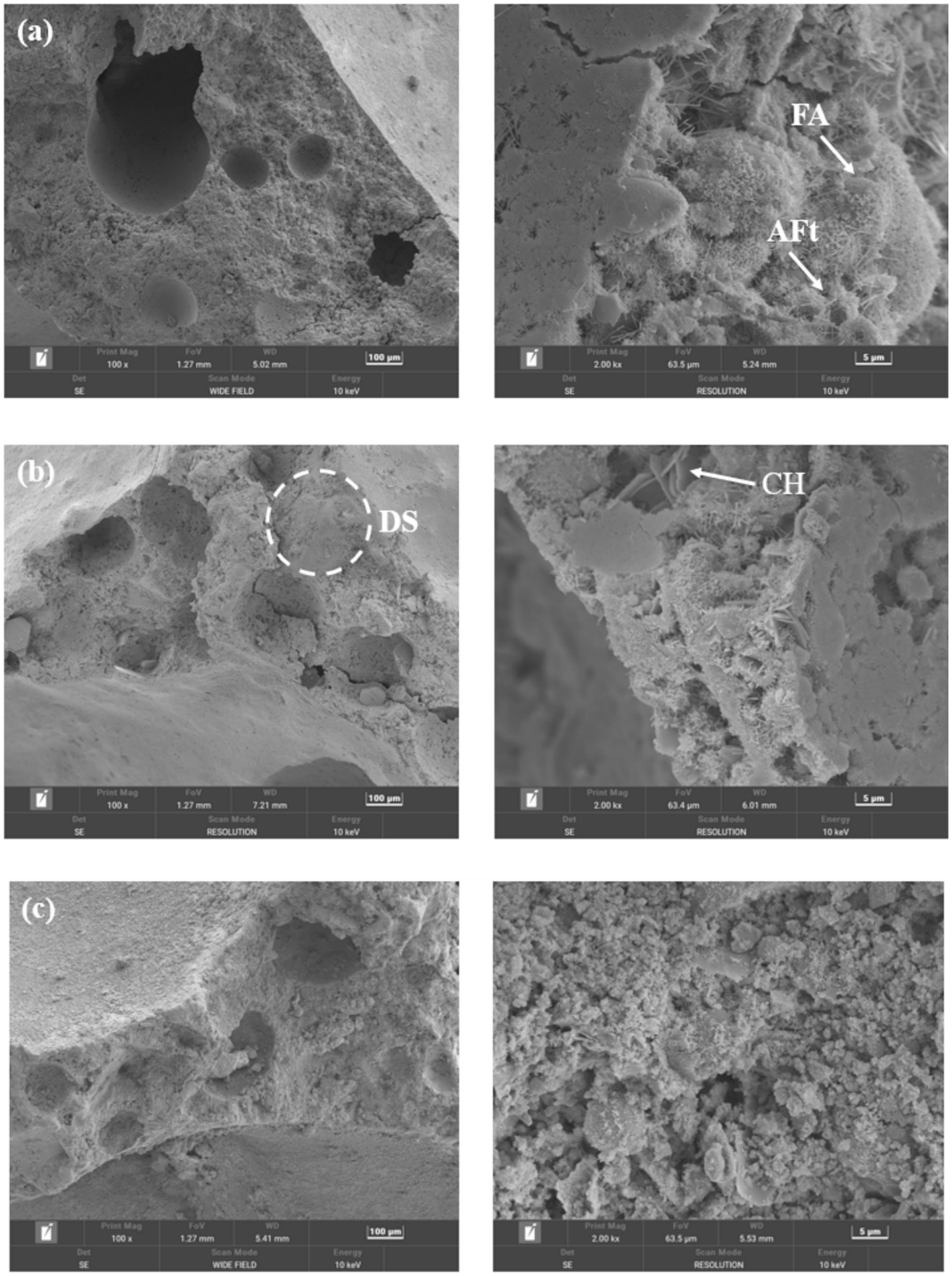

Fig. 16. SEM images of the DSFC matrix at 28 d. (a) DS0, (b) DS35, and (c) MR10.

$$S = \sqrt{2\pi c\rho\lambda/T} \tag{3}$$

$$D = \sum(S \times R) \tag{4}$$

Here, c is the specific heat capacity, kJ/(kg·K); λ is the thermal conductivity, W/(m·K); ρ is the dry density, kg/m^3, which are all obtained by testing. T is the period, generally 24 h; R is the thermal resistance, which can be obtained by Eq. (5), (m^2·K)/W.

$$R = H/\lambda \tag{5}$$

Where, H is the thickness of the foamed concrete board, m. According to previous studies, H is set to 20 mm.

Fig. 20 presents the thermal inertia index and heat storage coefficient of foamed concrete at 28 d. In general, a high heat storage coefficient represents an excellent heat insulation effect/heat storage capacity. With the increase of DS content, the heat storage coefficient increased significantly, which means that incorporating DS is beneficial to improve the heat insulation effect of buildings. After further incorporating RHA into the DSFC system, the heat storage coefficient of the samples decreased. This is different from thermal conductivity, which characterizes the heat preservation effect of foamed concrete. Meanwhile, DS and RHA had little effect on the thermal inertia index of DSFC samples, as shown in Fig. 20(b). With the increase of DS content, the

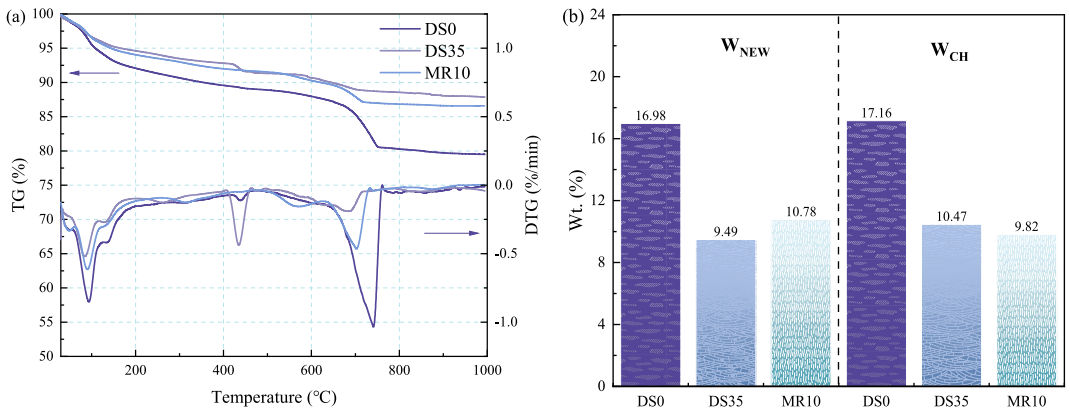

Fig. 17. The TGA results (a) and hydration product content (b) of the DSFC sample at 28 d.

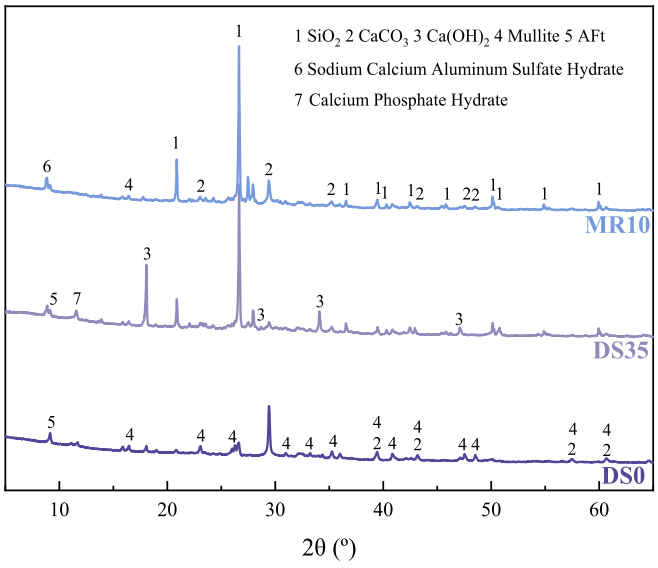

Fig. 18. XRD analysis of DSFC at 28 d.

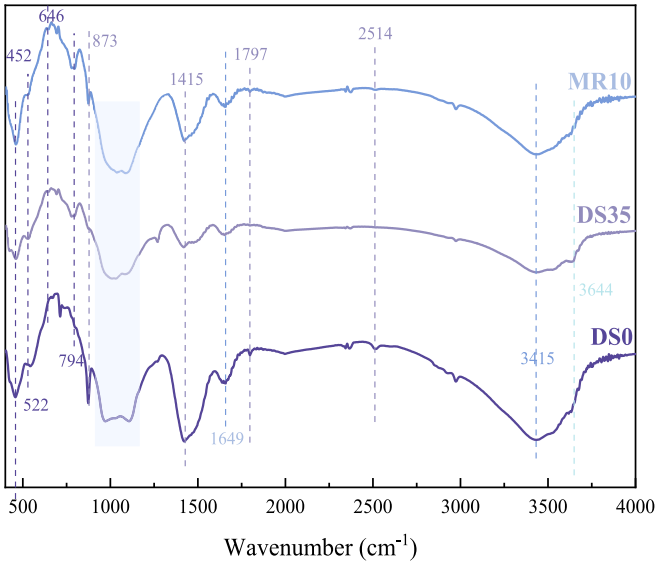

Fig. 19. FTIR spectra of DSFC at 28 d.

thermal inertia index slightly decreased, and the incorporation of RHA improved its thermal stability.

5.2. Economic and environmental benefit analysis

The cost and carbon emissions are key metrics for assessing the sustainability of building materials. Based on previous research, the environmental and economic benefits of binders are assessed by summing CO_2 emissions and costs of raw materials (see Table 3).

The results of the environmental and economic benefits of DSFC are shown in Table 4. Undoubtedly, the use of DS instead of binder to prepare DSFC is an effective way to reduce costs. With the increase in DS content, the total cost per cubic meter of DSFC was obviously reduced. When the substitution level of DS reached 50 %, the total cost per cubic meter of the mixture was reduced by 38.1 % relative to the control group. Meanwhile, as an agricultural waste, the cost of RHA is also low, which further reduces the cost of RHA-modified DSFC. The carbon footprint of the DS is also extremely low, with only the carbon emission of collection and transport being considered. The total carbon footprint per cubic meter of foamed concrete with 50 % DS was only about half that of the reference group. For better comparison, the ratio of total carbon emissions and cost per cubic meter to 28-d compressive strength was defined as the carbon emissions and cost per MPa per cubic meter. Compared to the reference mixture, the incorporation of DS resulted in an increase in the carbon footprint and cost per MPa per cubic meter of the mixture due to its reduction in mechanical strength. Incorporating an appropriate amount of RHA can effectively improve the economic and environmental benefits of the foamed mixture. The cost and CO_2 emission per MPa per cubic meter of the RHA-modified samples (5 %–10 %) were reduced by 20.3 %–39.1 % and 20.2 %–38.9 %, respectively, compared with the DS35 mixture.

The costs and carbon emissions of DSFCs are normalized, and its radar map is shown in Fig. 21. For high-volume DS-based foamed concrete, its CO_2 emissions and cost per unit strength are higher due to its strength reduction. Meanwhile, the RHA-modified DSFC performs the best in terms of cost and environmental aspects, both in terms of total amount and ratio to strength.

5.3. Performance comparison of Portland-based foamed concrete

Fig. 22 compares the basic properties of OPC-based foamed concrete. As presented in Fig. 22(a), as the density of foamed concrete increases, its 28-d compressive strength increases significantly. For high-density foamed concrete, it is more suitable for structural members, and their compressive strength can reach 10–90 MPa. High-strength foamed concrete tends to contain low foam content and high aggregate content [33]. To further reduce the density of foamed concrete, the researchers tried to reduce the aggregate content, especially the coarse aggregate

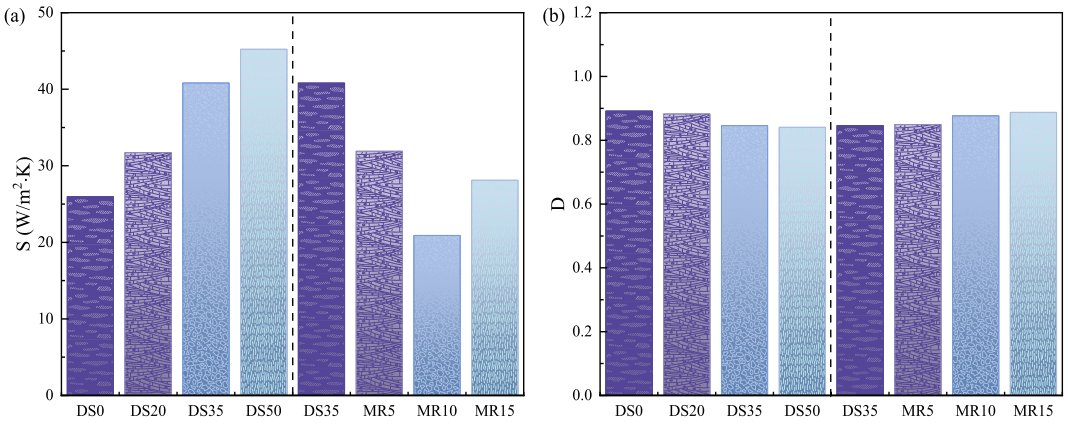

Fig. 20. The heat storage coefficient (a) and thermal inertia index (b) of DSFC.

Table 3
The CO_2-e emission and cost of raw materials.

Type	OPC	FA	RHA	DS
Cost (USD/ton)	84	37.5	15	6.18
CO_2-e emission (kg/kg)	0.821	0.009	0.1032	0.004
Ref.	[31]	[31]	[32]	[5]

Table 4
The cost and carbon footprint of the binder in mixtures.

MIX ID	Total cost per cubic meter (USD/m^3)	Total CE per cubic meter (kg/ m^3)	Cost per MPa per cubic meter (USD/m^3·MPa)	CE per MPa per cubic meter (kg/ m^3·MPa)
DS0	22.0995	0.1599	6.0824	0.0440
DS20	18.7296	0.1282	7.3933	0.0506
DS35	16.2022	0.1044	9.9197	0.0639
DS50	13.6748	0.0806	10.2561	0.0605
MR5	15.5545	0.1004	7.9091	0.0510
MR10	14.9061	0.0964	6.0430	0.0391
MR15	14.2581	0.0923	5.3468	0.0346

* CE: Carbon emission.

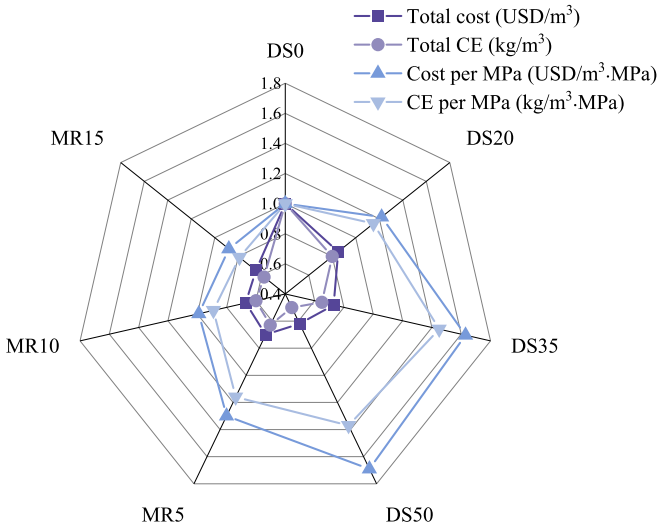

Fig. 21. The radar map of the economic and environmental benefits of the binder.

content. Some researchers use river sand, glass sand, and bottom sand in foamed concrete, which not only makes the bulk density of the sample higher but also the sedimentation of the sand affects the stability of the mixture [34–36]. To alleviate this problem, and to enhance the environmental and economic benefits of foamed concrete, this study modified the foamed mixture with DS with low density and small size. Compared with other sand-based foamed concrete, DSFC showed lower density, which makes it have a better thermal insulation ability.

The thermal conductivity of foamed concrete is another important indicator, and it increases with the increase of density as shown in Fig. 22(b). The chemical foaming method is one of the effective ways to prepare ultra-lightweight foamed concrete [21]. Pan et al. prepared chemically foamed concrete using hydrogen peroxide as a foaming agent with a dry density below 300 kg/m^3 and a thermal conductivity below 0.07 W/m·k [34]. However, the incorporation of aggregate increases the bulk density of the foamed concrete, which in turn increases its thermal conductivity. The foamed concrete prepared by Pan et al. contained ordinary sand, which made its thermal conductivity as high as 0.23–0.72 W/m·k [34]. Of course, the incorporation of sand also has a positive effect on foamed concrete. Gencel et al. added fine-sized glass sand to the foamed mixture and found that it effectively improved the strengths and durability of the samples [36]. Meanwhile, Gencel et al. also found that the strengths and durability of foamed concrete prepared with bottom lime sand and recycled fine aggregates were superior to those prepared with limestone sand [35]. The DS-based foamed concrete prepared in this study had a lower density, and it exhibited a relatively low thermal conductivity compared to foamed concrete with a similar density. In addition, the use of solid waste to replace part of the binder to prepare eco-friendly concrete is a common strategy. Lesovik et al. used FA and carbonate-siliceous rock to replace part of the OPC to increase the hardening rate of the mixture and improve its pore structure [39]. Meanwhile, Gökçe et al. also concluded that SF exhibited higher strength gain and durability improvement in foamed concrete compared to FA [43]. Therefore, the incorporation of SO_2-rich SCM into OPC-based foamed concrete may have a positive effect on its performance improvement. In addition, the improvement of the Y&P of the mixture by incorporating RHA is also the key to optimize its pore structure and thermal conductivity. Due to the significant density difference between the DS and the binder, this tends to destabilize the mixture. Therefore, increasing the viscosity of the mixture can effectively improve the sedimentation of DS. Properly increasing the yield stress of the mixture can improve the stability of the bubbles and improve the uniformity of DS in the foamed mixture.

6. Conclusions

An eco-friendly desert sand (DS)-based foamed concrete (DSFC) was developed, and rice husk ash (RHA) was used to further improve its

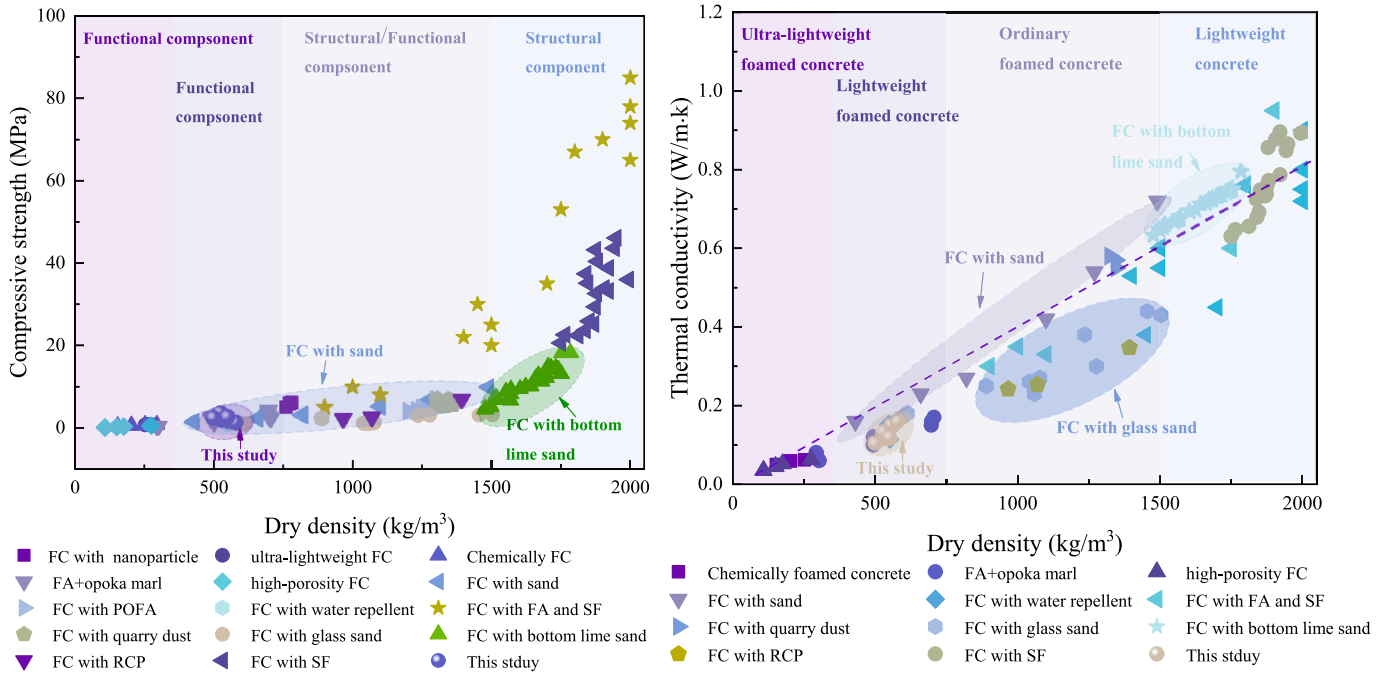

Fig. 22. Performance comparison of Portland-based foamed concrete. (a) Compressive strength and (b) Thermal conductivity [34–46].

performance. The hardening performance of DSFC was analyzed by the rheological properties of the fresh paste, and its feasibility from technical, economic, and environmental aspects were discussed. The main findings can be summarized as follows:

(1) The use of DS and RHA to replace cement and fly ash both resulted in reduced flowability of the mixture when the water/binder (OPC, FA, and RHA) ratio was constant. Due to the shear thinning effect, incorporating 20 % of DS decreased yield stress of the paste by 4.03 %, and the yield stress gradually increased with the further increase of DS content. Due to the porous nature and high specific surface area of RHA, the incorporation of 15 % RHA increased the yield stress of DS35 by 42.2 %.

(2) The incorporation of 50 % DS led to increasing the dry density and thermal conductivity of foamed concrete by 10.5 % and 39.9 %, respectively, which was related to the high density of DS and its disturbance to the pore structure of foamed concrete. Incorporating 10 % of lightweight and porous RHA into the DSFC mixture with 35 % DS reduced its dry density and thermal conductivity by 10.3 % and 30.9 %, respectively, which was also related to the improvement of the pore structure.

(3) The incorporation of low-reactivity DS resulted in a reduction in the cement content, which also resulted in a reduction in the strength and hydration product content of the foamed concrete. Meanwhile, RHA consumed CH in DSFC and then generated more C-S-H gel, which in combination with the improvement of pore structure increased the compressive strength of DSFC.

(4) The incorporation of 50 % DS reduced the content of the shrinkable components, thereby reducing by 37 % of the shrinkage deformation of the foamed concrete. Incorporating an appropriate amount of RHA also improved the pore structure of DSFC, which was also beneficial to reduce its shrinkage deformation.

(5) For the plain paste, high fluidity increased the large-sized pore content and pore interconnectivity. With incorporating 35 % DS, the porosity of the foamed concrete was reduced by 1.8 % due to the shearing effect of DS sinking in the mixture, but the pore homogeneity was greatly reduced. Further addition of 10 % RHA enhanced by 1.96 % of porosity of hardened samples by increasing the plastic viscosity of the mixture.

(6) Recycling DS and RHA in foamed concrete is an economical and eco-friendly strategy. The unit strength cost and carbon emission per cubic meter of the RHA-modified samples (5 %–10 %) were reduced by 20.3 %–39.1 % and 20.2 %–38.9 %, respectively, compared with the DS35 mixture. Meanwhile, the DSFC prepared in this study also exhibited an excellent performance compared to other Portland cement-based foamed concrete, which has a potential role as an external wall insulation material.

CRediT authorship contribution statement

Jinyan Shi: Formal analysis, Investigation, Writing – original draft. **Minghu Zhang:** Validation, Writing – review & editing. **Xuezhen Zhu:** Conceptualization, Writing – review & editing. **Çağlar Yalçınkaya:** Writing – review & editing. **Oğuzhan Çopuroğlu:** Writing – review & editing. **Yuanchun Liu:** Writing – review & editing, Funding acquisition.

Declaration of competing interest

None.

Data availability

Data will be made available on request.

Acknowledgments

This study was funded by the Heilongjiang Natural Science Foundation (No. LH2022E008).

References

[1] B. Bayrak, A. Benli, H.G. Alcan, O. Çelebi, G. Kaplan, A.C. Aydın, Recycling of waste marble powder and waste colemanite in ternary-blended green geopolymer composites: Mechanical, durability and microstructural properties, J. Build. Eng. 73 (2023) 106661.

[2] C. Liang, Y. Zhang, R. Wu, D. Yang, Z. Ma, The utilization of active recycled powder from various construction wastes in preparing ductile fiber-reinforced cementitious composites: A case study, Case Stud. Constr. Mater. 15 (2021) e00650.
[3] B. Pan, Y. Mao, S. Hou, C. Liang, Y. Gao, Corrosion mechanism of recycled mortar prepared from CO_2-treated hardened cement paste powder, Constr. Build. Mater. 384 (2023) 131321.
[4] L. Kai, X. Liu, X. Xie, R. Liu, T. Li, S.P. Shah, The feasibility of utilizing sifted desert sand (< 75 μm) as sustainable supplementary cementitious materials (SCM), Constr. Build. Mater. 406 (2023) 133375.
[5] M. Zhang, Z. Zhu, J. Shi, B. Liu, Z. He, C. Liang, Utilization of desert sand in the production of sustainable cement-based materials: A critical review, Construct. Build. Mater. 327 (2022) 127014.
[6] N.K. Ameta, A.S. Wayal, P. Hiranandani, Stabilization of Dune Sand with Ceramic Tile Waste as Admixture, Am. J. Eng. Res. 2 (2013) 133–139.
[7] K.R. Erzaij, R.H. Ali, The effect of desert environment on the cost of construction projects (materials transportation), Appl. Mech. Mater. 897 (2020) 152–156.
[8] S. Guettala, B. Mezghiche, Compressive strength and hydration with age of cement pastes containing dune sand powder, Construct. Build. Mater. 25 (2011) 1263–1269.
[9] Y. Li, H. Zhang, G. Liu, D. Hu, X. Ma, Multi-scale study on mechanical property and strength prediction of aeolian sand concrete, Construct. Build. Mater. 247 (2020) 118538.
[10] Z. He, B. Wang, W. Chen, H. Tao, Mechanical property, volume stability and microstructure of lightweight engineered cementitious composites (LECC) containing high-volume diatomite, Constr. Build. Mater. 409 (2023) 133884.
[11] H.M. Hamada, G.A. Jokhio, A.A. Alttar, F.M. Yahaya, K. Muthusamy, A. M. Humada, Y. Gul, The use of palm oil clinker as a sustainable construction material: A review, Cem. Concr. Comp. 106 (2020) 103447.
[12] S. Wang, H. Li, S. Son, Experimental research on a feasible rice husk/geopolymer foam building insulation material, Energ. Buildings 226 (2020) 110358.
[13] Z. Zhang, S. Liu, F. Yang, Y. Weng, S. Qian, Sustainable high strength, high ductility engineered cementitious composites (ECC) with substitution of cement by rice husk ash, J. Clean. Prod. 317 (2021) 128379.
[14] O. Gencel, A. Benli, O.Y. Bayraktar, G. Kaplan, M. Sutcu, W. Elabade, Effect of waste marble powder and rice husk ash on the microstructural, physico-mechanical and transport properties of foam concretes exposed to high temperatures and freeze-thaw cycles, Construct. Build. Mater. 291 (2021) 123374.
[15] P.A. Adesina, F.A. Olutoge, Structural properties of sustainable concrete developed using rice husk ash and hydrated lime, J. Build. Eng. 25 (2019) 100804.
[16] Z. He, L. Li, S. Du, Creep analysis of concrete containing rice husk ash, Cem. Concr. Comp. 80 (2017) 190–199.
[17] J. Wang, J. Xiao, Z. Zhang, K. Han, X. Hu, F. Jiang, Action mechanism of rice husk ash and the effect on main performances of cement-based materials: A review, Construct. Build. Mater. 288 (2021) 123068.
[18] J. Shi, J. Tan, B. Liu, J. Shi, Thermal and mechanical properties of thermal energy storage lightweight aggregate mortar incorporated with phase change material, J. Energy Storage. 32 (2020) 101719.
[19] O. Gencel, A. Yaras, G. Hekimoğlu, A. Ustaoglu, E. Erdogmus, M. Sutcu, A. Sarı, Cement based-thermal energy storage mortar including blast furnace slag/capric acid shape-stabilized phase change material: Physical, mechanical, thermal properties and solar thermoregulation performance, Energ. Buildings 258 (2022) 111849.
[20] C. Ma, B. Chen, Experimental study on the preparation and properties of a novel foamed concrete based on magnesium phosphate cement, Construct. Build. Mater. 137 (2017) 160–168.
[21] J. Shi, Y. Liu, H. Xu, Y. Peng, Q. Yuan, J. Gao, The roles of cenosphere in ultra-lightweight foamed geopolymer concrete (UFGC), Ceramics International. 48 (2022) 12884–12896.
[22] J. Shi, Y. Liu, B. Liu, D. Han, Temperature Effect on the Thermal Conductivity of Expanded Polystyrene Foamed Concrete: Experimental Investigation and Model Correction, Adv. Mater. Sci. Eng. 1 (2019) 2379.
[23] J. Shi, Y. Liu, E. Wang, L. Wang, C. Li, Physico-mechanical, thermal properties and durability of foamed geopolymer concrete containing cenospheres, Construct. Build. Mater. 325 (2022) 126841.
[24] A.H. Amir, Experimental investigations on the physical and rheological characteristics of sand-foam mixtures, J. Non-Newton. Fluid. 221 (2015) 28–39.
[25] Y. Xie, J. Li, Z. Lu, J. Jiang, Y. Niu, Effects of bentonite slurry on air-void structure and properties of foamed concrete, Construct. Build. Mater. 179 (2018) 207–219.
[26] A. Alhozaimy, M.S. Jaafar, A. Abdullah, Y.H. Taufiq-Yap, Properties of high strength concrete using white and dune sands under normal and autoclaved curing, Construct. Build. Mater. 27 (2012) 218–222.
[27] M. Mollah, W. Yu, R. Schennach, D.L. Cocke, A Fourier transform infrared spectroscopic investigation of the early hydration of Portland cement and the influence of sodium lignosulfonate, Cement Concr. Res. 30 (2000) 267–273.
[28] G. Voicu, G. Tiuca, A. Badanoiu, A. Holban, Nano and mesoscopic SiO_2 and ZnO powders to modulate hydration, hardening and antibacterial properties of portland cements, J. Build. Eng. 57 (2022) 104862.
[29] R. Ylmén, U. Jäglid, B. Steenari, I. Panas, Early hydration and setting of Portland cement monitored by IR, SEM and Vicat techniques, Cement Concr. Res. 39 (2009) 433–439.
[30] H. Zhang, J. Yang, H. Wu, P. Fu, W. Yang, Dynamic thermal performance of ultra-light and thermal-insulative aerogel foamed concrete for building energy efficiency, Solar Energy. 204 (2020) 569–576.
[31] Y. Nie, J. Shi, Z. He, B. Zhang, Y. Peng, Y. Lu, Evaluation of high-volume fly ash (HVFA) concrete modified by metakaolin: Technical, economic and environmental analysis, Powder Technol. 397 (2022) 7121.
[32] E. Ozturk, C. Ince, S. Derogar, R. Ball, Factors affecting the CO_2 emissions, cost efficiency and eco-strength efficiency of concrete containing rice husk ash: A database study, Construct, Build. Mater. 326 (2022) 126905.
[33] O. Gencel, M. Nodehi, O.Y. bayraktar, G. Kaplan, A. Benli, A. Gholampour, T. Ozbakkaloglu,, Basalt fiber-reinforced foam concrete containing silica fume: An experimental study, Construct, Build. Mater. 326 (2022) 126861.
[34] Z. Pan, F. Hiromi, T. Wee, Preparation of High Performance Foamed Concrete from Cement, Sand and Mineral Admixtures, Journal of Wuhan University of Technology (materials Science Edition). 2 (2007) 295–298.
[35] O. Gencel, B. Balci, O.Y. Bayraktar, M. Nodehi, A. Sari, The effect of limestone and bottom ash sand with recycled fine aggregate in foam concrete, J. Build. Eng. 54 (2022) 104689.
[36] O. Gencel, O.Y. Bayraktar, G. Kaplan, O. Arslan, Lightweight foam concrete containing expanded perlite and glass sand: Physico-mechanical, durability, and insulation properties, Construct. Build. Mater. 320 (2022) 126187.
[37] Z. Huang, T. Zhang, Z. Wen, Proportioning and characterization of Portland cement-based ultra-lightweight foam concretes, Construct. Build. Mater. 79 (2015) 390–396.
[38] Z. Pan, H. Li, W. Liu, Preparation and characterization of super low density foamed concrete from Portland cement and admixtures, Construct. Build. Mater. 72 (2014) 256–261.
[39] V. Lesovik, V. Voronov, E. Glagolev, R. Fediuk, A. Baranov, Improving the behaviors of foam concrete through the use of composite binder, J. Build. Eng. 31 (2020) 101414.
[40] J. Jiang, Z. Lu, Y. Niu, J. Li, Y. Zhang, Study on the preparation and properties of high-porosity foamed concretes based on ordinary Portland cement, Mater. Design. 92 (2016) 949–959.
[41] A.M. Alnahhal, U.J. Alengaram, S. Yusoff, R. Singh, W. Deboucha, Synthesis of sustainable lightweight foamed concrete using palm oil fuel ash as a cement replacement material, J. Build. Eng. 35 (2021) 2047.
[42] C. Ma, B. Chen, Properties of foamed concrete containing water repellents, Construct. Build. Mater. 123 (2016) 106–114.
[43] H.S. Gökçe, D. Hatungimana, K. Ramyar, Effect of fly ash and silica fume on hardened properties of foam concrete, Construct. Build. Mater. 194 (2019) 1–11.
[44] S.K. Lim, C.S. Tan, B. Li, T. Ling, Utilizing high volumes quarry wastes in the production of lightweight foamed concrete, Construct. Build. Mater. 151 (2017) 441–448.
[45] O. Gencel, M. Nodehi, G. Hekimolu, A. Ustaolu, A. Sar, Foam Concrete Produced with Recycled Concrete Powder and Phase Change Materials, Sustainability. 14 (2022) 1–25.
[46] O. Gencel, M. Nodehi, O.Y. Bayraktar, G. Kaplan, A. Benli, Basalt fiber-reinforced foam concrete containing silica fume: An experimental study, Construct. Build. Mater. 326 (2022) 126861.